IOPscience iopscience.iop.org

Home Search Collections Journals About Contact us My IOPscience

Influence of Si and N additions on structure and phase stability of $Ge_2Sb_2Te_5$ thin films

This article has been downloaded from IOPscience. Please scroll down to see the full text article.

2009 J. Phys.: Condens. Matter 21 435501

(http://iopscience.iop.org/0953-8984/21/43/435501)

View the table of contents for this issue, or go to the journal homepage for more

Download details:
IP Address: 129.252.86.83
The article was downloaded on 30/05/2010 at 05:36

Please note that terms and conditions apply.

J. Phys.: Condens. Matter **21** (2009) 435501 (8pp) doi:10.1088/0953-8984/21/43/435501

Influence of Si and N additions on structure and phase stability of $Ge_2Sb_2Te_5$ thin films

Helmut Kölpin[1], Denis Music[1], Galyna Laptyeva[2], Reza Ghadimi[2], Florian Merget[3], Silvia Richter[2], Ruslàn Mykhaylonka[1], Joachim Mayer[2] and Jochen M Schneider[1]

[1] Materials Chemistry, RWTH Aachen University, D-52056 Aachen, Germany
[2] Central Facility for Electron Microscopy, RWTH Aachen University, Ahornstraße 55, D-52074 Aachen, Germany
[3] Institute of Semiconductor Electronics, RWTH Aachen University, Sommerfeldstraße 24, D-52074 Aachen, Germany

Received 16 July 2009, in final form 17 September 2009
Published 9 October 2009
Online at stacks.iop.org/JPhysCM/21/435501

Abstract
The influence of Si and N in $Ge_2Sb_2Te_5$ (space group $Fm\bar{3}m$) on structure and phase stability thereof was studied experimentally by thin film growth and characterization as well as theoretically by *ab initio* calculations. It was found that Si and N most probably accumulate in the amorphous matrix embedding $Ge_2Sb_2Te_5$ grains. The incorporation of Si and N in these samples causes an increase of the crystallization temperature and the formation of finer grains. N is more efficient in increasing the crystallization temperature and in reducing the grain size than Si which can be understood based on the bonding analysis. The incorporation of both Si and N in $Ge_2Sb_2Te_5$ is energetically unfavourable, leading to finer grains and larger crystallization temperatures. While in the case of Si additions no significant changes in bonding are observed, N additions appear to enable the formation of strong Te–N bonds in the amorphous matrix, which are shown to be almost twice as strong as the strongest bonds in unalloyed $Ge_2Sb_2Te_5$.

1. Introduction

$Ge_2Sb_2Te_5$ is a chalcogenide phase, which can rapidly and reversibly be switched between the amorphous and crystalline state through thermal or inductive heating [1, 2]. With a heating rate of $10\,^{\circ}\mathrm{C\,min^{-1}}$ unalloyed, amorphous $Ge_2Sb_2Te_5$ was reported to crystallize at 142 °C and to form a metastable cubic phase (space group $Fm\bar{3}m$ [3]), which transforms at 240 °C to a stable hexagonal phase and finally melts at 616 °C [1]. The amorphous and cubic $Ge_2Sb_2Te_5$ possesses different optical and electrical properties. Significant differences in optical properties of $Ge_2Sb_2Te_5$ were reported for wavelengths in the infrared and red spectral ranges [1]. The electrical resistivity of amorphous $Ge_2Sb_2Te_5$ is 2–3 orders of magnitude larger compared to cubic $Ge_2Sb_2Te_5$ [4]. In combination with its phase change behaviour, GeSbTe is applicable for phase change memory devices. It is already in use for optical data discs, based on the changes in its optical properties [5–7] and was proposed to be a promising candidate for electronic non-volatile memory devices [8, 9]. In these devices, the phase change is triggered by electrical impulses, which is accompanied by a change in electrical resistivity and utilized to store bits of information [10]. A short electrical pulse of low voltage, e.g. a 1 ns pulse with 1.5 V [11], which heats the GeSbTe to a temperature between its crystallization and melting temperature, leads to crystallization of the GeSbTe, while a long pulse of larger voltage, e.g. a 50 ns pulse with 4 V [11], is needed to heat the GeSbTe above the melting temperature for reamorphization [8, 11].

Tailoring the switching properties of $Ge_2Sb_2Te_5$ may be carried out by the addition of other elements. Si [12–14] and N [15] were proposed to be promising candidates as additional elements in $Ge_2Sb_2Te_5$ and were the focus of several studies. The resistivity of the crystalline state can be increased by addition of both Si and N and therefore a lower RESET current, which is related to the crystalline–amorphous phase transition, is necessary to trigger the phase change by an electrical pulse. Feng *et al* investigated the switching ability

 © 2009 IOP Publishing Ltd Printed in the UK

of $Ge_2Sb_2Te_5$ with additions of N and Si and reported that only the samples with Si additions have the capability to perform SET and RESET cycles in contrast to $Ge_2Sb_2Te_5$ with N additions, which exhibits no RESET capability [16]. Moreover, it was reported that the activation energy for nucleation [17–19], the thermal stability and the crystallization temperature ($T_{cryst.}$) increase with the increase in the amount of the N and Si additions [12, 13, 18, 20]. Furthermore, it was reported for $Ge_2Sb_2Te_5$ with additions of N that the crystallinity decreases [16, 21, 22] and the crystal size is reduced [22–24]. Even though $Ge_2Sb_2Te_5$ with additions of N and Si has been studied extensively, and the causality between chemical composition and crystallization temperature as well as grain size has been reported, the underlying physical and chemical mechanisms are not fully understood.

It was claimed that phase separation occurs so that Si and N agglomerate in grain boundaries [19, 24] or form an additional amorphous phase [16, 18, 25]. However, no energetics or electronic structure data have been reported for these two sections. Furthermore, Coombs *et al* have studied the effect of Se, S, Sn and Si in $Ge_{39}Sb_9Te_{52}$ and report a linear correlation between the nucleation time and the bond energy [25], which may imply that stronger bonds in amorphous $Ge_2Sb_2Te_5$ lead to an increased activation energy. In $Ge_2Sb_2Te_5$ with additions of N, Ge–N bonds were suggested to form [21, 26, 27]. However, it is still not clear how N and Si are bonded in $Ge_2Sb_2Te_5$.

In order to contribute towards understanding the influence of Si and N additions on structure and phase stability of $Ge_2Sb_2Te_5$, we carry out structural analysis on crystallized $Ge_2Sb_2Te_5$ thin films containing up to 18.0 and 10.5 at.% of Si and N, respectively. Parallel to these investigations, *ab initio* calculations are performed to study the energetics and the bonding nature of unalloyed $Ge_2Sb_2Te_5$ and $Ge_2Sb_2Te_5$ with Si and N additions.

The results presented here are consistent with the notion of phase separation during crystallization. It is shown that the formation of unalloyed $Ge_2Sb_2Te_5$ is energetically more favourable as compared to the here investigated Si or N alloyed configurations. Therefore, during annealing Si and N may accumulate in the amorphous phase, while $Ge_2Sb_2Te_5$ forms crystals. Moreover, it can be learned that N may form two times stronger bonds with Te compared to the strongest bonds in unalloyed $Ge_2Sb_2Te_5$, which may explain both the more pronounced grain refinement and the increase of the crystallization temperature for $Ge_2Sb_2Te_5$ with N additions as compared with unalloyed $Ge_2Sb_2Te_5$.

2. Experimental methods

600 nm $Ge_2Sb_2Te_5$ thin films with N and Si were synthesized by magnetron sputtering, applying an additional 50 nm interlayer at the substrate–film interface and a 250 nm capping layer to inhibit nucleation of crystalline $Ge_2Sb_2Te_5$ and oxidation thereof, respectively. Due to the different chemical nature of these additions and characterization requirements, Al_2O_3 was used as an interlayer and capping layer in the case of both N and Si additions, while TiO_2 interlayer and capping was only applied for samples that were characterized by transmission electron microscopy because the samples with an Al_2O_3 capping layer cracked during sample preparation. A $Ge_2Sb_2Te_5$ compound target was used for the deposition of the $Ge_2Sb_2Te_5$ layer of all samples under the same conditions. The target normal was perpendicular to the substrate surface. The distance between the plasma source and the substrate was 80 mm. A pulsed DC generator with a frequency of 50 kHz and an off time of 1 ns with a constant power density of 4.9 $W\ cm^{-2}$ was employed. The base pressure was of the order of 1×10^{-7} mbar and the working pressure during all depositions was held constant at 7.1×10^{-3} mbar. $Ge_2Sb_2Te_5$ with Si was synthesized by combinatorial DC sputtering with an Si target aligned at an angle of 42° to the sample normal at a distance of 80 mm and power densities of 0.4, 0.8, 1.5 and 3.0 $W\ cm^{-2}$. $Ge_2Sb_2Te_5$ with N was grown by reactive sputtering with a gas mixture of argon and nitrogen, varying the nitrogen fraction from 1% to 20%. The Al_2O_3 and TiO_2 layers were deposited *in situ* by reactive DC sputtering, applying pure Al and Ti targets, a constant power density of 0.8 $W\ cm^{-2}$, a base pressure of 1×10^{-7} mbar, a working pressure of 3.0×10^{-3} mbar including 5% oxygen in the argon atmosphere, at a working distance of 190 mm.

After deposition, all films were annealed in air. During this process, the crystallization progress was monitored through the measurement of the relative reflectivity of the samples using an infrared camera [4]. They were heated by applying a heating rate of 0.022 73 $K\ s^{-1}$ in the case of $Ge_2Sb_2Te_5$ with Si and 0.0076 $K\ s^{-1}$ for $Ge_2Sb_2Te_5$ with N. All samples were heated up to the crystallization point, except for the samples with high Si concentration, which were heated up to a maximum temperature of 250 °C. These heating rates were chosen with the intention of reaching the crystallization point and under the limitation of our equipment (250 °C).

The chemical composition of the crystalline $Ge_2Sb_2Te_5$ layers was measured with electron probe microanalysis (EPMA). To analyse the structure of the $Ge_2Sb_2Te_5$ samples, x-ray diffraction (XRD) with an area detector and high resolution transmission electron microscopy (HRTEM) using a FEI Tecnai F20 operated at 200 kV were carried out. The samples for HRTEM were prepared out of the crystallized samples using a focused ion beam (FEI Strata FIB 205).

3. Theoretical methods

The theoretical investigations in this work were performed employing the density functional theory [28]. The generalized-gradient approximation (GGA) [29, 30] and projector augmented wave potentials [31] with Blöchl corrections for the total energy [32] were applied in all calculations. A k-point grid of $7 \times 7 \times 7$ determined after Monkhorst–Pack [33] was utilized for the integration in the Brillouin zone within an energy cutoff of 500 eV and these calculations were processed until the convergence criterion for the total energy of 0.01 meV was reached. The computer program used was the Vienna *ab initio* simulation package (VASP) [31]. The cubic $Ge_2Sb_2Te_5$ structure was treated using the hexagonal description as introduced by Sun *et al* [34]. One unit cell

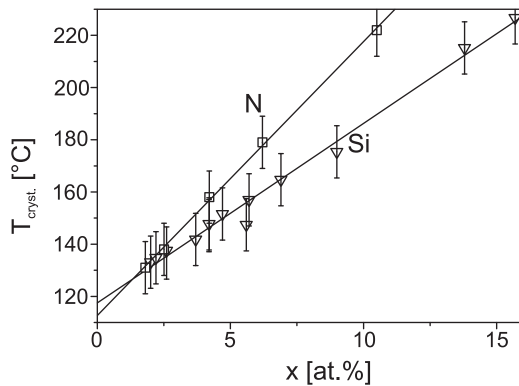

Figure 1. Crystallization temperature ($T_{cryst.}$) as a function of the Si and N content (x).

contains 27 atoms with 6 Ge and Sb atoms as well as 15 Te atoms. One additional element (Si or N) was incorporated at all possible substitutional or interstitial sites as described below. For all calculations, the internal free parameters (atomic positions) in a unit cell were relaxed first and then the lattice constants, i.e. a and c (hexagonal description of cubic $Ge_2Sb_2Te_5$), were calculated. The energy of formation was calculated with respect to unalloyed elemental phases, which were obtained in the same manner as described above with the following space groups: $Im\bar{3}m$ for Si and Ge, $R\bar{3}m$ for Te and Sb, N as a molecule.

4. Results and discussion

The chemical composition analysis of the annealed films revealed that the Si and N concentration increases from 2.0 to 18.0 at.% and from 1.8 to 10.5 at.%, respectively. Figure 1 shows the crystallization temperature ($T_{cryst.}$) as a function of the N and Si content of the $Ge_2Sb_2Te_5$ samples, measured during annealing by the reflectivity measurements. The crystallization temperature increases from 132 °C for $Ge_2Sb_2Te_5$ with 2.0 at.% Si up to 227 °C for $Ge_2Sb_2Te_5$ with 15.7 at.% Si and from 131 °C for $Ge_2Sb_2Te_5$ with 1.8 at.% N up to 222 °C for $Ge_2Sb_2Te_5$ with 10.5 at.% N. Comparing linear data fits, the slope belonging to the $Ge_2Sb_2Te_5$ with N is 10.5 °C per at.% N while the corresponding slope of $Ge_2Sb_2Te_5$ with Si is only 6.9 °C per at.% Si. This indicates that the influence of N in $Ge_2Sb_2Te_5$ compared to Si on the $T_{cryst.}$ is 1.5 times larger. The influence of the interfaces on the $T_{cryst.}$ was the same for all samples, since the same capping and interlayer phase (Al_2O_3) was used. Therefore, the estimated difference of the $T_{cryst.}$ for unalloyed $Ge_2Sb_2Te_5$ of the order of 10 °C (intercept of $T_{cryst.}$ at $x = 0$) may be attributed to the different heating rates. Comparing the crystallization temperature for pure $Ge_2Sb_2Te_5$ as obtained by differential scanning calorimetry [1] and the estimate made by extrapolation of our data at $x = 0$, a deviation of approximately 25 °C is observed, which may be due to different experimental methods used. Since the heating rate for $Ge_2Sb_2Te_5$ with N was smaller than the one for $Ge_2Sb_2Te_5$ with Si, the slope for $Ge_2Sb_2Te_5$ with N is slightly underestimated, while the slope for $Ge_2Sb_2Te_5$ with Si is thus slightly overestimated. Furthermore, slower heating rates may give rise to more precise data. Despite the different heating rates employed here we can conclude that the influence of N on $T_{cryst.}$ is stronger than for Si additions.

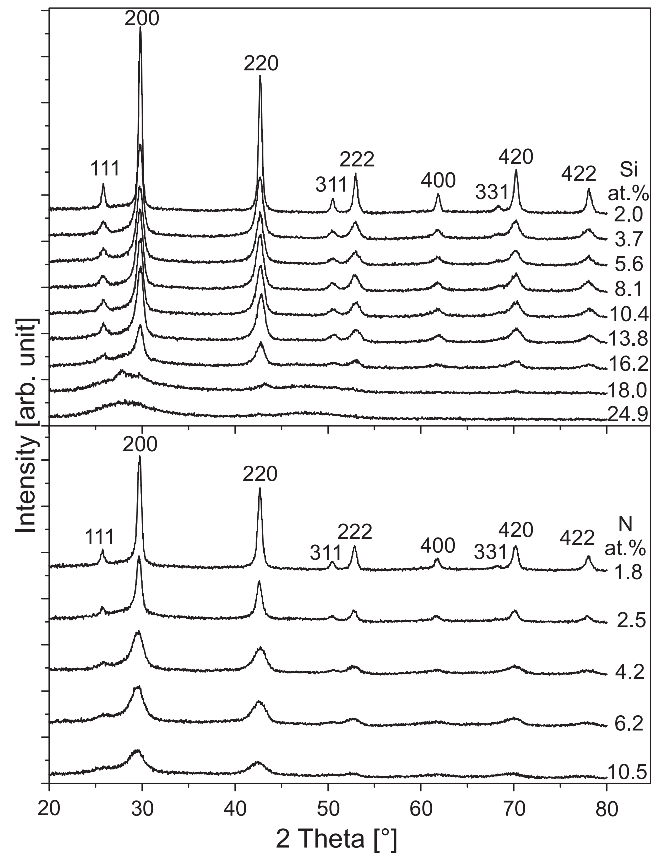

Figure 2. XRD data of $Ge_2Sb_2Te_5$ with additions of Si (upper panel) and with additions of N (lower panel).

In order to identify the structure of the annealed samples, we analysed XRD data which are shown in figure 2. The upper panel contains the data for the $Ge_2Sb_2Te_5$ samples with Si and the lower panel the data for the $Ge_2Sb_2Te_5$ samples with N. All samples exhibit cubic structure ($Fm\bar{3}m$) except for $Ge_2Sb_2Te_5$ with 18.0 at.% Si, where only some indications for crystallization are present, and the amorphous $Ge_2Sb_2Te_5$ sample with 24.9 at.% Si, because the $Ge_2Sb_2Te_5$ samples with Si were only annealed up to 250 °C. The lattice parameter a of the cubic structure is with 6.00 ± 0.01 Å not a function dependent on the chemical composition. The peak intensities are decreasing with increasing Si and N content, indicating that the amount of the cubic crystalline phase is decreasing, while a larger amount of the samples remains amorphous during annealing. These results are consistent with the notion that phase separation occurs and Si and N agglomerate in an additional amorphous phase (matrix) during annealing [16, 18, 25]. Based on the Debye–Scherrer method [35], the grain sizes were determined from the diffraction data and presented in figure 3 as a function of the content of Si and N. The grain sizes are decreased as the N and Si concentration is increased. The data on N-induced grain size

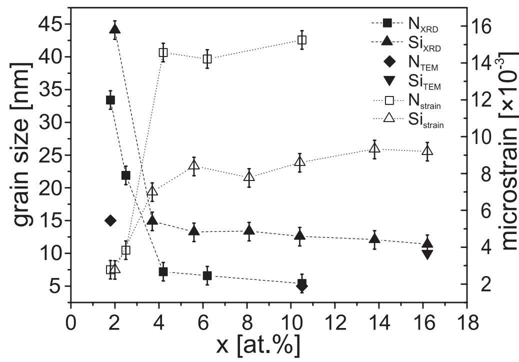

Figure 3. Grain size and microstrain as a function of the N and Si content (x), based on XRD and TEM measurements.

reduction is consistent with the literature [22–24]. Moreover, N additions promote finer grains as compared to Si additions. The suppressed grain growth may be explained by the N-and Si-enriched amorphous matrix which hinders the grain growth. The finer grains in the samples with N may indicate that the grain growth in the N-enriched amorphous matrix is stronger suppressed as compared to the Si-enriched amorphous matrix. Therefore, we analyse the electronic structure thereof in the text below.

If the method of Keijser *et al* [36] is applied to estimate the grain size including microstrain evaluation as shown in figure 3, the increase of N from 1.8 to 10.5 at.% and Si from 2.0 to 16.2 at.% leads to a decrease in grain size and an increase of the microstrain from 0.002 to 0.015 and from 0.002 to 0.009, respectively. The most significant change occurs at <4 at.%. This increase of the microstrain with the increasing Si and N content supports the notion of phase separation, because a higher driving force is needed to promote grain growth, which implies increased stresses in the lattice. In order to corroborate the observations based on XRD, HRTEM images of several samples are presented in figure 4, including the samples with 1.8 at.% N, 16.2 at.% Si and 10.5 at.% N. The fast Fourier-transformation data are provided in the left corner of the HRTEM micrographs. These data clearly reveal the cubic $Ge_2Sb_2Te_5$ structure, which is consistent with the XRD analysis. The Fourier-transformation filtered images presented in the right panel may be used to resolve the amorphous matrix of the samples (darker area) and the crystallites (lighter areas). Apparently, all $Ge_2Sb_2Te_5$ samples contain an amorphous matrix. Also unalloyed, crystallized $Ge_2Sb_2Te_5$ contains an amorphous matrix, as is reported in the literature [37]. This finding is consistent with the assumption that Si and N may accumulate in the amorphous matrix. The approximate grain sizes for $Ge_2Sb_2Te_5$ with 1.8 at.% N, 16.2 at.% Si and 10.5 at.% N shown in figure 3 are 15, 10 and 5 nm, respectively. They are somewhat smaller than the mean grain sizes calculated by the Debye–Scherrer method using the XRD data (see figure 3). This may be explained by the small sample sections, investigated by HRTEM, combined with the fact that grains were superimposed with an amorphous matrix in the volume investigated. Other reasons may be due to HRTEM sample preparation. The composition-induced

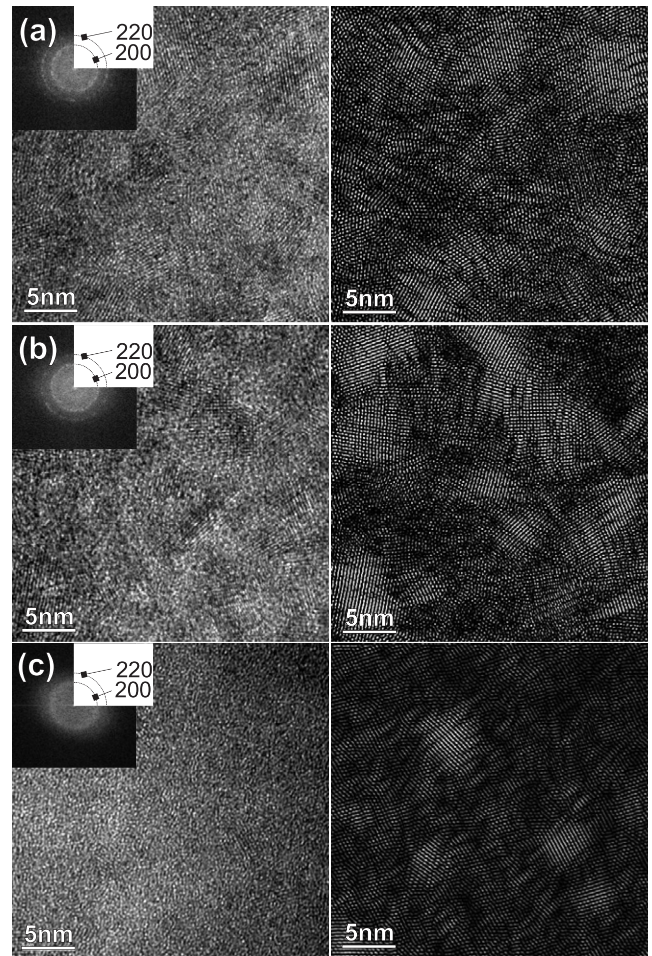

Figure 4. HRTEM images of $Ge_2Sb_2Te_5$ with N and Si additions: (a) $Ge_2Sb_2Te_5$ with 1.8 at.% N, (b) $Ge_2Sb_2Te_5$ with 16.2 at.% Si and (c) $Ge_2Sb_2Te_5$ with 10.5 at.% N. The left panel includes the HRTEM image and fast Fourier-transformed image (corner), while the right panel is the Fourier-transformation filtered image to point out the crystalline areas.

variation obtained based on XRD data is supported by the HRTEM data.

Ab initio calculations were performed to study energetics and the bonding nature of unalloyed $Ge_2Sb_2Te_5$ and $Ge_2Sb_2Te_5$ including Si and N additions in order to identify the cause of the above described causality between N and Si additions to $Ge_2Sb_2Te_5$ and the grain size as well as the crystallization temperature. A $Ge_2Sb_2Te_5$ unit cell as used for these investigations is shown in figure 5. $Ge_2Sb_2Te_5$ possesses a stacking sequence of Te–Ge–Te–Sb–Te–v–Te–Sb–Te–Ge– in the [111] direction, where v represents an ordered vacancy layer [34]. The highlighted area, including three Te atoms (termed Te(1), Te(2), Te(3)), one Sb and Ge atom and a vacancy, represents one of the rigid building blocks. An additional element, Si or N, can be placed at one of the sites, termed sub 'atom' and occ v as shown in figure 6. Also, four possible octahedral sites (termed o 'atom'–'atom') are shown in figure 6, being the first set of the interstitial sites investigated. The remaining sites, i.e. all possible tetrahedral sites (termed t 'atom', triple-nearest neighbour–'atom', single-

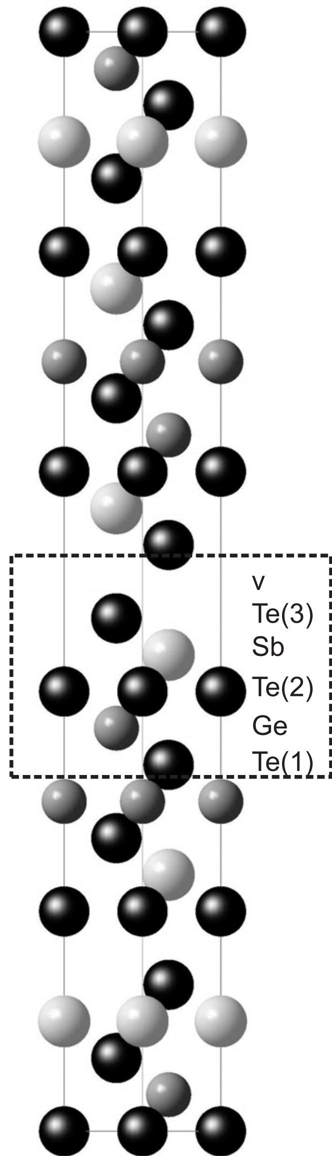

Figure 5. $Ge_2Sb_2Te_5$ unit cell, where black spheres designate Te, white Sb and grey Ge sites. The highlighted area represents one of the rigid building blocks.

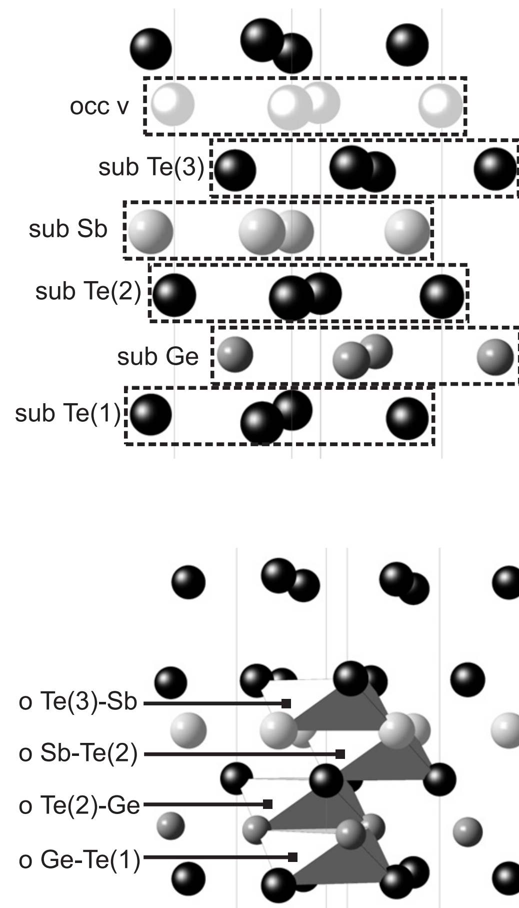

Figure 6. Rigid building blocks of the $Ge_2Sb_2Te_5$ unit cell showing the substitutional sites (termed sub 'atom'), octahedral sites (termed o 'atom'–'atom') and the vacancy site (termed occ v).

Table 1. The energy of formation E_{form} and lattice constants of the hexagonal description of the cubic $Ge_2Sb_2Te_5$ cell (a_{hex} and c_{hex}) and of the cubic cell ($a_{fcc\ by\ a}$ and $a_{fcc\ by\ c}$) calculated using a_{hex} and c_{hex} for unalloyed $Ge_2Sb_2Te_5$ and $Ge_2Sb_2Te_5$ with Si or N.

Phase	a_{hex} (Å)	c_{hex} (Å)	$a_{fcc\ by\ a}$ (Å)	$a_{fcc\ by\ c}$ (Å)	E_{form} (meV/atom)
Unalloyed $Ge_2Sb_2Te_5$	4.28	52.85	6.05	6.10	−113.3
Si sub Ge	4.27	52.04	6.04	6.01	−87.4
Si sub Sb	4.24	52.26	6.00	6.03	−83.0
N t Ge–Te(1)	4.27	53.51	6.18	6.04	−6.6
N t Sb–Te(2)	4.27	53.46	6.17	6.03	−17.6
N t Sb–Te(3)	4.25	53.46	6.17	6.01	−13.7

nearest neighbour) are presented in figure 7. The N and Si content in all calculations is equal to 3.7 at.% for the substitutional sites and 3.6 at.% in the case of the interstitial sites. Table 1 contains the theoretical results, including the lattice parameters of the hexagonal description of the cubic $Ge_2Sb_2Te_5$ (a_{hex} and c_{hex}) and the corresponding cubic cell data obtained from a_{hex} and c_{hex} ($a_{fcc\ by\ a}$ and $a_{fcc\ by\ c}$) as well as the energy of formation (E_{form}) of unalloyed $Ge_2Sb_2Te_5$ and $Ge_2Sb_2Te_5$ with N and Si additions at the most stable sites. The deviation between the calculated and measured lattice parameter is less than 1.6%. This is consistent with our previously presented notion of phase separation where the crystalline $Ge_2Sb_2Te_5$ phase is almost unalloyed.

It is well known that GGA overestimates lattice constants [38, 39]. The calculated lattice constants of $Ge_2Sb_2Te_5$ are in good agreement with the experiment and previous calculations by Sun *et al* [40]. It has to be noted that adding Si and N affects the lattice constants only marginally. Therefore, it is not possible to exclude the possibility that Si or N may be incorporated by analysing the lattice constants only. In order to critically evaluate the notion of phase separation, it is more meaningful to probe the energetics by studying the energy of formation with respect to the elements. Unalloyed $Ge_2Sb_2Te_5$ is energetically more favourable as compared to $Ge_2Sb_2Te_5$ alloyed with Si or N. The energy of formation of $Ge_2Sb_2Te_5$ with Si or N is approximately 30 or 110 meV/atom

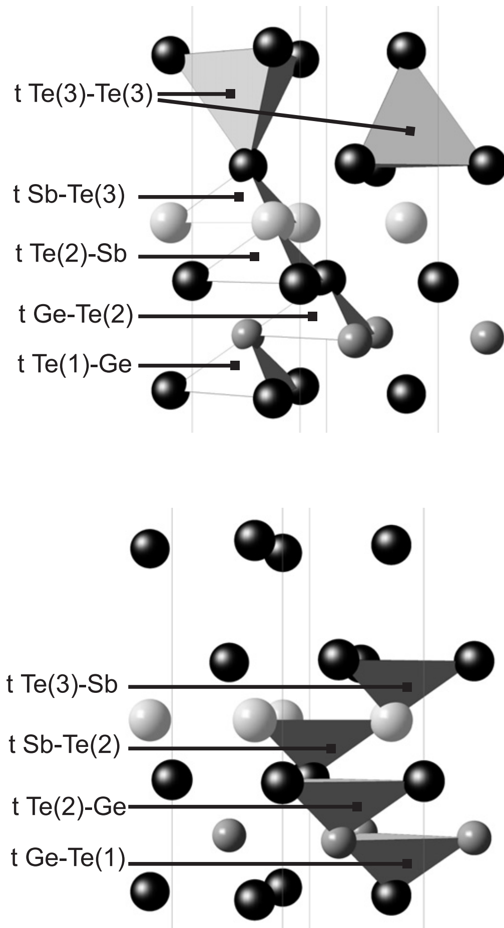

Figure 7. Rigid building blocks of the $Ge_2Sb_2Te_5$ unit cell showing the tetrahedral sites. These sites are termed t 'atom'–'atom', where t 'atom' designates a triple-nearest neighbour and 'atom' stands for a single-nearest neighbour. For instance, t Te(1)–Ge describes a tetrahedral site formed by three Te(1) atoms and one Ge atom.

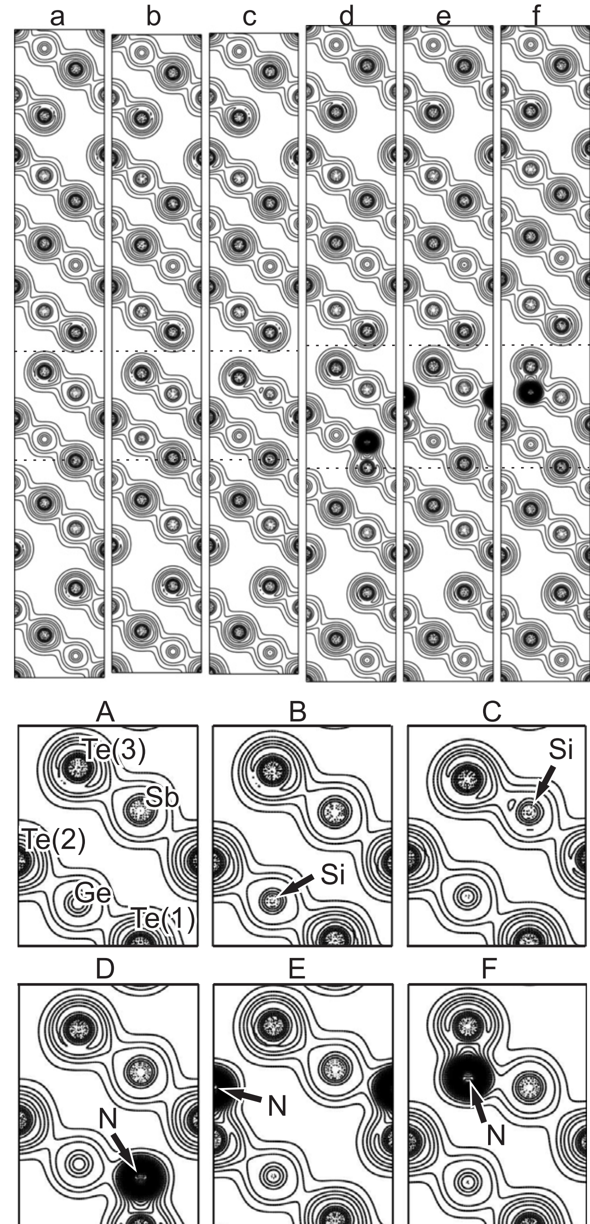

Figure 8. Electron density distribution of (a) unalloyed $Ge_2Sb_2Te_5$, ((b) and (c)) $Ge_2Sb_2Te_5$ with 3.7 at.% Si (Ge; Sb substituted), ((d)–(f)) $Ge_2Sb_2Te_5$ with 3.6 at.% N (t Ge–Te(1), t Sb–Te(2), t Sb–Te(3)). The capital letters show the rigid building block where Si and N were introduced of the corresponding phase. The electron density distribution increases from −0.5 to 0.6 au ((a)–(c)) and from −0.5 to 3.7 au ((d)–(f)).

larger compared to unalloyed $Ge_2Sb_2Te_5$, respectively (see table 1). However, Si and N may be incorporated into the $Ge_2Sb_2Te_5$ lattice during sputtering due to the non-equilibrium character of this synthesis technique, preferentially at Ge or Sb sites and at tetrahedral sites, respectively. If Si is incorporated in $Ge_2Sb_2Te_5$ as in the case of our experiment by simply adding Si to unalloyed $Ge_2Sb_2Te_5$, without removing the element to be substituted, phase separations may occur. We propose the following reactions for incorporation of one Si atom into a $Ge_2Sb_2Te_5$ unit cell at the most stable positions:

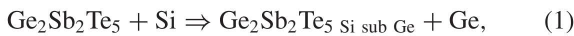

$$Ge_2Sb_2Te_5 + Si \Rightarrow Ge_2Sb_2Te_{5\ \mathrm{Si\ sub\ Ge}} + Ge, \qquad (1)$$

$$Ge_2Sb_2Te_5 + Si \Rightarrow Ge_2Sb_2Te_{5\ \mathrm{Si\ sub\ Sb}} + Sb \qquad (2)$$

and for N:

$$Ge_2Sb_2Te_5 + N_2/2 \Rightarrow Ge_2Sb_2Te_{5\ \mathrm{N\ t\ Sb-Te(2)}}. \qquad (3)$$

The energies needed to facilitate these reactions are 769, 777 and 4270 meV/atom, respectively. Hence, the unalloyed $Ge_2Sb_2Te_5$ structure is energetically more favourable, implying that the unalloyed $Ge_2Sb_2Te_5$ phase should form during annealing supporting the notion of phase separation. This is consistent with our experimental data.

To investigate the different behaviour of N and Si concerning the grain size and the crystallization temperature, the electron density distribution was studied further. The electron density distributions of the most stable $Ge_2Sb_2Te_5$ configurations, with and without additions of Si and N, are shown in figure 8. Since the structure model used for $Ge_2Sb_2Te_5$ is based on stacking of the rigid building blocks [34] as discussed above, it is expected that this notion is reflected in the electronic structure. We observe Te–Ge

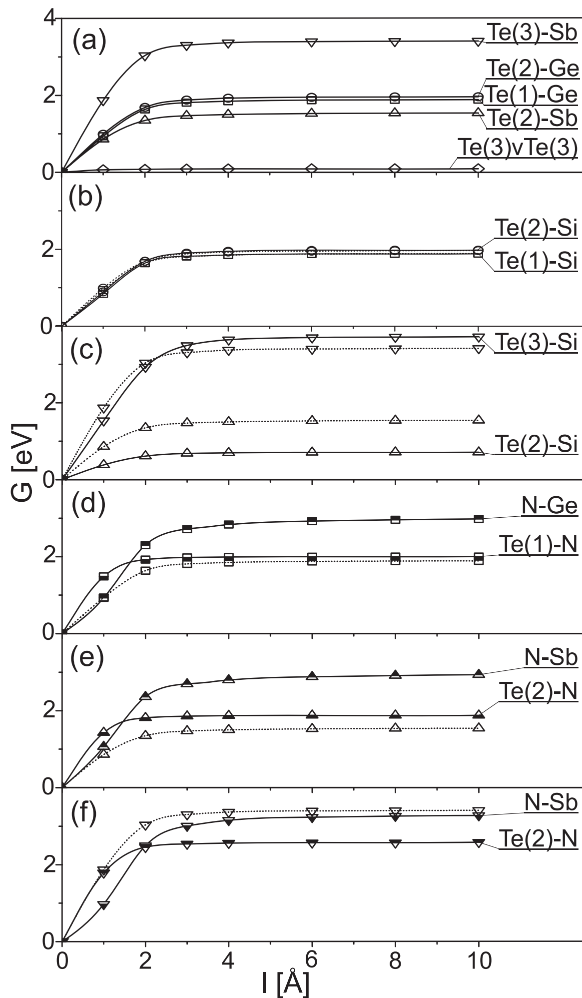

Figure 9. Decohesion energy (G) as a function of the phase separation distance (l) at a certain c plane for (a) unalloyed $Ge_2Sb_2Te_5$, ((b) and (c)) $Ge_2Sb_2Te_5$ with 3.7 at.% Si (Ge; Sb substituted), ((d)–(f)) $Ge_2Sb_2Te_5$ with 3.6 at.% N (t Ge–Te(1), t Sb–Te(2), t Sb–Te(3)). The dashed lines designate the corresponding decohesion data of unalloyed $Ge_2Sb_2Te_5$.

and Te–Sb units, which are characterized by the sharing of electrons. This is consistent with strong covalent bonding in these units. These data are also consistent with the density of states presented previously [40]. The electronic structure seems to be almost unaffected by Si. This implies that the bonds which Si forms in $Ge_2Sb_2Te_5$ are similar to the ones formed in unalloyed $Ge_2Sb_2Te_5$. However, N obviously forms strong bonds with Te (not primarily with Ge or Sb) if it is incorporated at the most stable tetrahedral sites. To study the bonds in more detail, the decohesion energy G was calculated for every c plane in unalloyed $Ge_2Sb_2Te_5$. It is defined herein as the energy needed to separate the structure into two blocks. No structural relaxations were allowed during the phase separation. The bond energy can be estimated by dividing the decohesion energy by the number of bonds in the plane. Figure 9 summarizes the results obtained in this study. In unalloyed $Ge_2Sb_2Te_5$, the largest decohesion energy is 3.421 eV. This plane contains 3 Te(3)–Sb bonds so that the Te(3)–Sb bond energy is 1.140 eV/bond. The lowest decohesion energy of 0.093 eV is obtained if the cell is divided between Te(3) and Te(3). Investigation of the $Ge_2Sb_2Te_5$ with Si reveals that the bond energy of the Te(1)–Ge/Si and Te(2)–Ge/Si remains almost unaffected. Moreover, if Si substitutes Sb, the corresponding bond energy is influenced by less than 50%. If N is incorporated into $Ge_2Sb_2Te_5$, striking differences with respect to the bond energy occur. Taking into account that there is only one Te–N bond per unit cell, the bond energy is 1.880 up to 2.583 eV/bond, meaning that the bond energy is approximately twice as large as the strongest bond in unalloyed $Ge_2Sb_2Te_5$. These strong Te–N bonds could explain the different behaviour of N and Si concerning the grain size and the crystallization temperature. As the system approaches equilibrium (during annealing), Si and N may accumulate in the amorphous matrix. The strong interactions between N and Te may explain the grain refinement and the larger increase of the crystallization temperature for $Ge_2Sb_2Te_5$ with N, because the grain growth is hindered and more thermal energy is needed in order to form nuclei in amorphous $Ge_2Sb_2Te_5$. Si, not exhibiting any strong interaction with the other elements in $Ge_2Sb_2Te_5$, leads to a smaller increase of the crystallization temperature combined with less fine grains.

5. Conclusions

We have studied the influence of N and Si additions in $Ge_2Sb_2Te_5$ on structure and phase stability of sputtered thin films. The effect of Si and N positions in the $Ge_2Sb_2Te_5$ lattice on the stability and bonding was studied theoretically by *ab initio* calculations. The Si and N concentration in the annealed films was varied from 2.0 to 18.0 at.% and from 1.8 to 10.5 at.%, respectively. The crystallization temperature was increased and the grain size was decreased by adding Si and N to $Ge_2Sb_2Te_5$. The influence of N on the crystallization temperature is 1.5 times larger than for Si. The crystalline phase possesses, independently of the Si and N concentrations, the NaCl structure with no significant changes in lattice parameter. This is consistent with the notion of phase separation in an amorphous Si-rich and N-rich matrix, respectively, where an increase of the Si and N content leads to finer grains. This effect is more pronounced for N than for Si. This causality may be understood based on *ab initio* data. The formation of unalloyed $Ge_2Sb_2Te_5$ is energetically more favourable as compared to the here investigated Si or N alloyed configurations based on the energy of formation data. These data are consistent with the notion of phase separation in an amorphous Si-rich and N-rich matrix. Si and N may be incorporated into the $Ge_2Sb_2Te_5$ lattice under non-equilibrium conditions, preferentially at Ge or Sb sites and at tetrahedral sites, respectively. Si and N show only marginal influence on the lattice parameters. Si in $Ge_2Sb_2Te_5$ changes the bond energy to its nearest neighbours by less than 50%, as compared to those existing in unalloyed $Ge_2Sb_2Te_5$, but N exhibits two times stronger bonds with Te compared with the strongest bonds in unalloyed $Ge_2Sb_2Te_5$. Hence, as the system approaches equilibrium (during annealing) Si and N may accumulate in the amorphous matrix. The strong interactions between N and Te may explain the more

pronounced grain refinement and the larger increase of the crystallization temperature for $Ge_2Sb_2Te_5$ with N additions as compared to Si additions.

Acknowledgments

Support granted by the DFG (German Research Foundation) is gratefully acknowledged. For the grain size and microstrain measurements, K Jiang is gratefully acknowledged.

References

[1] Yamada N, Ohno E, Nishiuchi K and Akahira N 1991 *J. Appl. Phys.* **69** 2849
[2] Welnic W, Pamungkas A, Detemple R, Steimer C, Blügel S and Wutting M 2006 *Nat. Mater.* **5** 56
[3] Nonaka T, Ohbayashi G, Toriumi Y, Mori Y and Hashimoto H 2000 *Thin Solid Films* **370** 258
[4] Kim D, Merget F, Bolivar P H and Kurz H 2005 *J. Appl. Phys.* **97** 083538
[5] Kolobov A V, Fons P, Tominaga J, Frenkel A I, Ankudinov A L, Yannopoulos S N, Andrikopoulos K S and Uruga T 2005 *Japan. J. Appl. Phys.* **44** 3346
[6] Maeda T, Terao M and Shimano T 2003 *Japan. J. Appl. Phys.* **42** 1044
[7] Ohta T, Nishiuchi K, Narumi K and Kitaoka Y 2000 *Japan. J. Appl. Phys.* **39** 770
[8] Yin Y, Miyachi A, Niida D, Sone H and Hosaka S 2006 *Japan. J. Appl. Phys.* **45** 3238
[9] Goronkin H and Yang Y 2004 *MRS Bull.* **29** 805
[10] Nakayama K, Kojima K, Hayakawa F, Imai Y, Kitagawa A and Suzuki M 2000 *Japan. J. Appl. Phys.* **39** 6157
[11] Chao D-S, Lien C, Lee C-M, Chen Y-C, Yeh J-T, Chen F, Chen M-J, Yen P H, Kao M-J and Tsai M-J 2008 *Appl. Phys. Lett.* **92** 062108
[12] Qiao B, Feng J, Lai Y, Lin Y, Tang T, Cai B and Chen B 2006 *Appl. Surf. Sci.* **252** 8404
[13] Qiao B, Feng J, Lai Y, Ling Y, Lin Y, Tang T, Cai B and Chen B 2006 *Chin. Phys. Lett.* **23** 172
[14] Cai Y, Zhou P, Lin Y, Tang T, Chen L, Li J, Qiao B, Lai Y, Feng J, Cai B and Chen B 2007 *Chin. Phys. Lett.* **24** 781
[15] Yeh T, Hsieh T and Shieh H D 2004 *Japan. J. Appl. Phys.* **43** 5316
[16] Feng J, Zhang Y, Qiao B W, Lai Y F, Lin Y Y, Cai B C, Tang T A and Chen B 2007 *Appl. Phys.* A **87** 57
[17] Ling Y, Lin Y, Qiao B, Lai Y, Feng J, Tang T, Cai B and Chen B 2006 *Japan. J. Appl. Phys.* **45** L349
[18] Feng J, Zang Z F, Cai B C, Lin Y Y, Tang T A and Chen B 2007 *J. Appl. Phys.* **101** 074502
[19] Hu D Z, Lu X M, Zhu J S and Yan F 2007 *J. Appl. Phys.* **102** 113507
[20] Privitera S, Rimini E and Zonca R 2004 *Appl. Phys. Lett.* **85** 3044
[21] Kim Y, Jeong K, Cho M, Hwang U, Jeong H S and Kim K 2007 *Appl. Phys. Lett.* **90** 171920
[22] Seo H, Jeong T, Park J, Yeon C and Kim S 2000 *Japan. J. Appl. Phys.* **39** 745
[23] Takase A, Fujinawa G, Ebina A, Hirasaka M and Sugiyama I 2002 *Japan. J. Appl. Phys.* **41** 2189
[24] Jeong T H, Kim M R, Seo H, Park J W and Yeon C 2000 *Japan. J. Appl. Phys.* **39** 2775
[25] Coombs J H, Jongenelis A P J M, van Es-Spiekman W and Jacobs B A J 1995 *J. Appl. Phys.* **78** 4918
[26] Kim Y, Jang M H, Jeong K, Cho M, Do K H, Ko D, Sohn H C and Kim M G 2008 *Appl. Phys. Lett.* **92** 061910
[27] Liu B, Song Z, Zhang T, Xia J, Feng S and Chen B 2005 *Thin Solid Films* **478** 49
[28] Hohenberg P and Kohn W 1964 *Phys. Rev.* **136** B864
[29] Perdew J P 1991 *Electronic Structure of Solids '91* ed P Ziesche and H Eschrig (Berlin: Akademie Verlag) p 11
[30] Perdew J P and Wang Y 1992 *Phys. Rev.* B **45** 13244
[31] Kresse G and Joubert D 1999 *Phys. Rev.* B **59** 1758
[32] Bloechl P E 1994 *Phys. Rev.* B **50** 17953
[33] Monkhorst H J and Pack J D 1976 *Phys. Rev.* B **13** 5188
[34] Sun Z, Zhou J and Ahuja R 2006 *Phys. Rev. Lett.* **96** 055507
[35] Patterson A L 1939 *Phys. Rev.* **56** 978
[36] de Keijser Th H, Langford J I, Mittemeijer E J and Vogels A B P 1982 *J. Appl. Cryst.* **15** 308
[37] Park Y J, Lee J Y, Youm M S, Kim Y T and Lee H S 2005 *J. Appl. Phys.* **97** 093506
[38] van de Walle A and Ceder G 1999 *Phys. Rev.* B **59** 14992
[39] Fuchs M, Da Silva J L F, Stampfl C, Neugebauer J and Scheffler M 2002 *Phys. Rev.* B **65** 245212
[40] Sun Z, Kyrsta S, Music D, Ahuja R and Schneider J M 2007 *Solid State Commun.* **143** 240